The University of Nottingham

UNITED KINGDOM · CHINA · MALAYSIA

DEPARTMENT OF ELECTRICAL AND ELECTRONIC ENGINEERING

EEEE3075 / Mechatronics Laboratory

Lab 1 Simulink Experiment:

DC Motor PID Control

Name: Jason Samuel Pangestu

Student ID: 16522575

Table of Content

Figure List

Introduction

A DC Motor was one of the primary motors that were used for robotic system application. In this report, a Brushed Permanent Magnet DC motor will be investigated since we just need to control the input voltage to rotate in clockwise or anti-clockwise direction, unlike the brushless DC motors that were hard to control [1]. The investigation will lead to build a state-space model of Brushed Permanent Magnet DC Motor using Simulink and integrated the plant with PID controller by tuning the PID values to achieve the required response. The first step was to model the equations of electro-mechanical system. These models and related equations will be explained in method section. From this model, the state-space form will be used to generate function blocks. These function blocks will be formed and arranged based on open-loop system in Simulink. In this system, the plant will be tested and the waveforms of the current, angular velocity, and angular displacement will be simulated and analysed. For the close-loop system, the desired response was set to 1 and the PID values (Controller) need to be adjusted to make sure that the actual response generated 1 after going through the plant model. The overall system diagram can be seen from the figure 1 below.

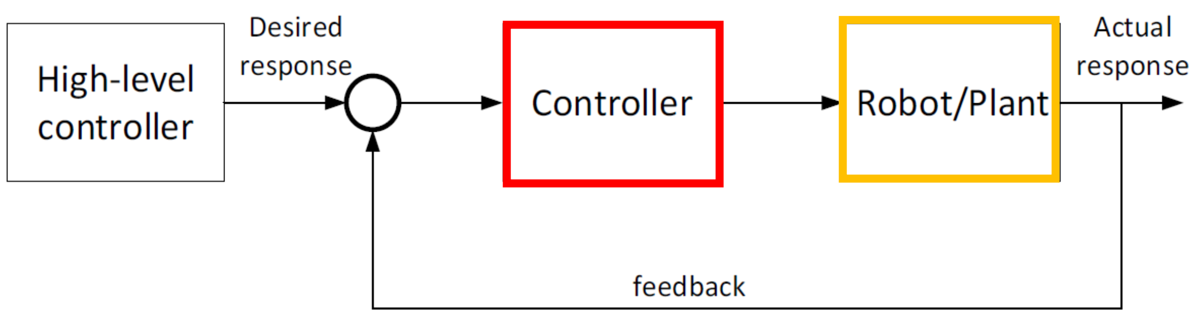

Figure 1 Close loop System Diagram

Methods

In this section, the function blocks which will be put in the Simulink were derived from the standard equations.

The Motor Equation was introduced:

$$V_{in} = L\frac{di}{dt} + Ri + k_e\omega \qquad \textit{(Eqn1)}$$

Where: Vin is the input voltage, L is the motor inductance, R is the resistance, k_e is the back emf constant, ω is the angular velocity, and i is the motor current.

The Motion Equation was introduced:

$$J\ddot{\theta} + c\dot{\theta} = T_m - T_{load} \qquad \textit{(Eqn2)}$$

Where: J is the equivalent inertia, c is the equivalent viscous damping, T_m is the motor input torque, T_{load} is the other load from the system, $\ddot{\theta}$ is the angular acceleration, and $\dot{\theta}$ is the angular velocity.

In this report, the J formula is:

$$J = J_{motor} + \frac{J_{robot}}{G^2} \qquad \textit{(Eqn3)}$$

Where: J_{motor} is the motor inertia, J_{robot} is the robot inertia, and G is the gear ratio

From equation (2), T_m can be substituted with $k_m i$

$$T_m = k_m i \qquad \textit{(Eqn4)}$$

Where: k_m is the motor torque constant and i is the motor current

Combines System Model Equation was introduced:

From equation (1), (2), and (3), the electrical and dynamic relationships were illustrated by the equations below;

$$J\ddot{\theta} + c\dot{\theta} - k_m i = -T_{load} \qquad \textit{(Eqn5)}$$

$$L\frac{di}{dt} + Ri + k_e\dot{\theta} = V_{in} \qquad \textit{(Eqn6)}$$

State-Space Form Equations were introduced:

From equations (5) and (6), the state space equations need to be formed by considering the 3 output variables (Angular displacement (θ), angular velocity ($\dot{\theta}$), and motor current (i)). Each of the variable ($x_1 = \theta$, $x_2 = \dot{\theta}$, $x_3 = i$) was substituted from equations (5), (6) and will result in first order ODE.

$$\dot{x}_1 = x_2 \quad \textit{(Eqn7)}$$

$$\dot{x}_2 = -\frac{c}{J}x_2 + \frac{k_m}{J}x_3 - T_{load} \quad \textit{(Eqn8)}$$

$$\dot{x}_3 = -\frac{k_e}{L}x_2 - \frac{R}{L}x_3 + \frac{V_{in}}{L} \quad \textit{(Eqn9)}$$

Block-Diagram Form equation was introduced:

Tload from equation (8) was neglected since the simulation will not take input from any external load. Next, the state-space form equations were transformed to Laplace equations and then transformed to block diagram equations.

$$sx_1 = x_2$$

$$\frac{x_1}{x_2} = \frac{1}{s} \quad \textit{(Eqn7)}$$

$$sx_2 = -\frac{c}{J}x_2 + \frac{k_m}{J}x_3 - T_{load}$$

$$\frac{x_2}{x_3} = \frac{k_m}{Js+c} \quad \textit{(Eqn8)}$$

$$sx_3 = -\frac{k_e}{L}x_2 - \frac{R}{L}x_3 + \frac{V_{in}}{L}$$

$$\frac{x_3}{V_{in}-k_e x_2} = \frac{1}{Ls+R} \quad \textit{(Eqn9)}$$

These three equations (7,8,9) were transformed to block diagrams and were arranged similar with the figure below. The left-hand side of each of the equation is the output (numerator) and input (denominator).

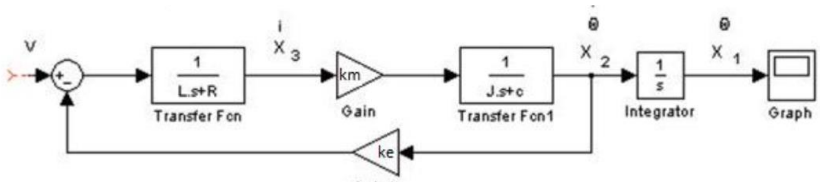

Figure 2 Open Loop System for DC Motor Plant

Analysis and Results

1. Open-loop model using Simulink

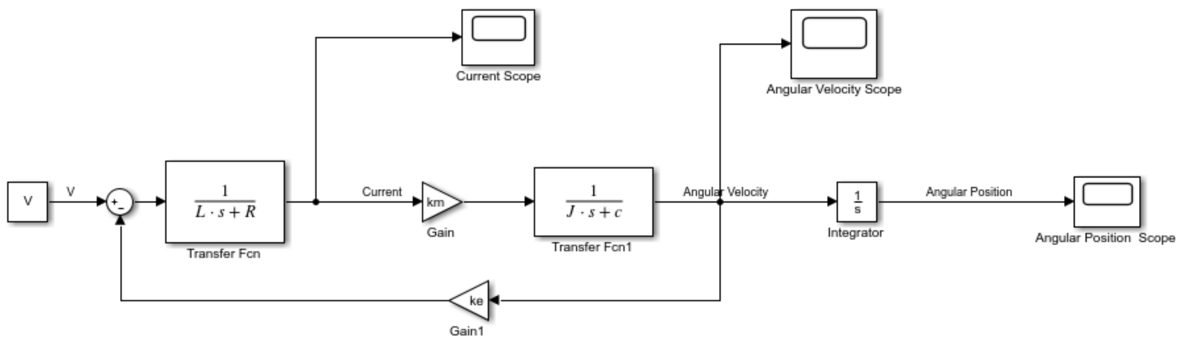

Figure 3 Open Loop System of DC Motor

Explanation for each function of the block:

From figure 3, the explanation will be started from the left of the diagram. The square block with the name “V” is a constant block. In this diagram, the block provided the input voltage signal of 12V for the plant. Next to the right, the round shape with + and – sign is the sum block (it can add or subtract input). In this case, the positive input is the 12V voltage signal and the negative input is the gain of ke “Gain1”. The output of this sum will be transferred to the “Transfer Fcn”. At the bottom side, the triangular shape name “Gain1” is a gain block which multiply the value from the “Transfer Fcn1” and will go to sum block. This gain block has a back emf constant value (ke). At the top side, we can see the “Transfer Fcn”. This is the transfer function block that is related with equation 9 *(Eqn9)*, hence the output is current. At the right side, the triangular shape name “Gain” is a gain block which multiply the value from the “Transfer Fcn” to “Transfer Fcn1”. This gain block has a motor torque constant value (km). At the right side, it is shown the “Transfer Fcn1”. This is the transfer function block that is related with equation 8 *(Eqn8)*, hence the output is angular velocity. At the right side, we can see an integrator block that is related with equation 7 (*Eqn7*). The function of this block is to calculate the value of the integral of its input signal with respect to time. In this case, the output of this block is the angular position. Furthermore, it can be seen from figure 3 that there are 3 scopes (Current, angular velocity, and angular position scope) that will be analysed.

a. Without changing the payload mass ($5kg$) and the motor inertia ($1.3 \times 10^{-4} kgm^2$)

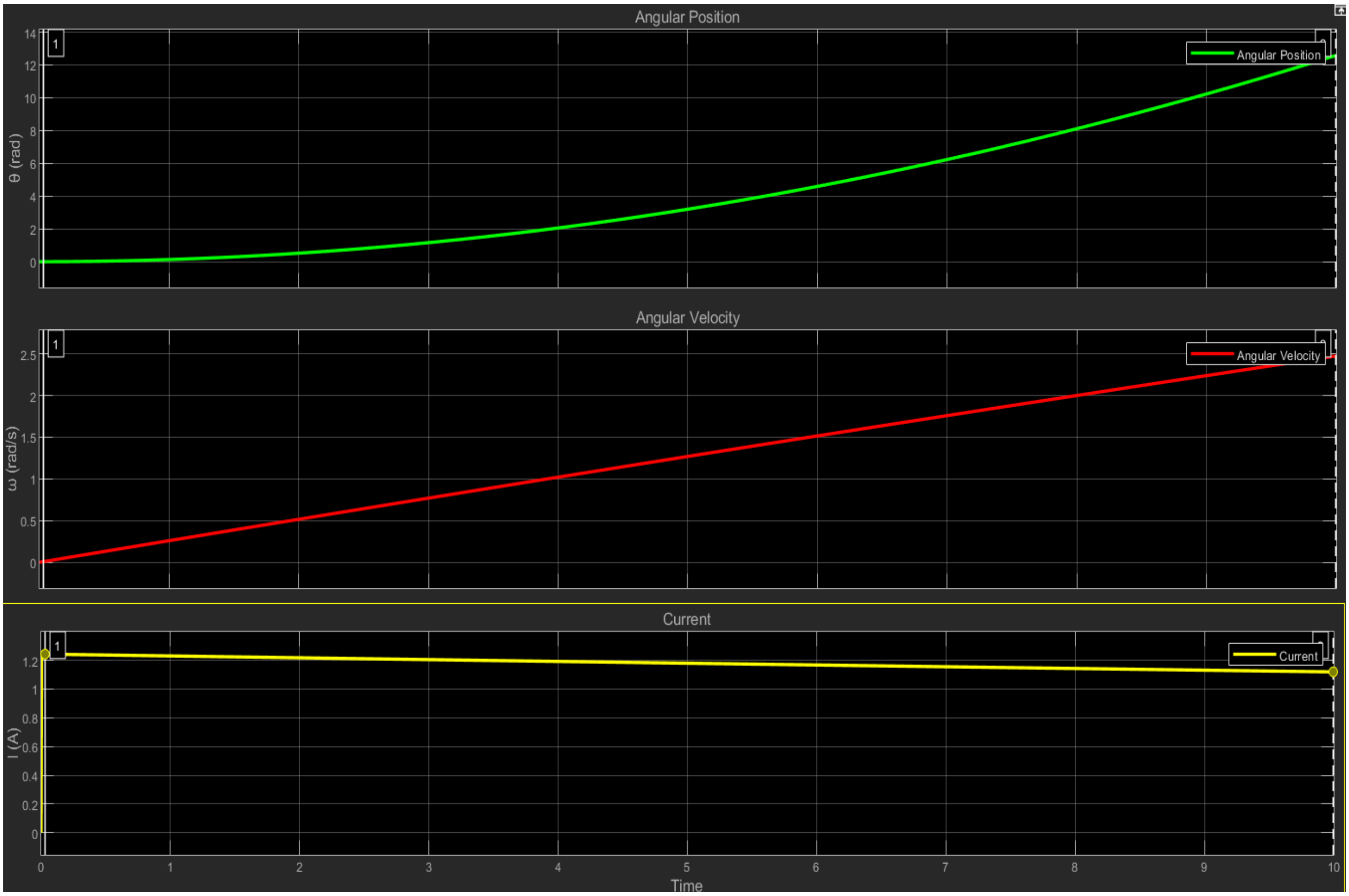

Figure 4 Waveforms of Angular Position, Angular velocity, and Current for 10 seconds

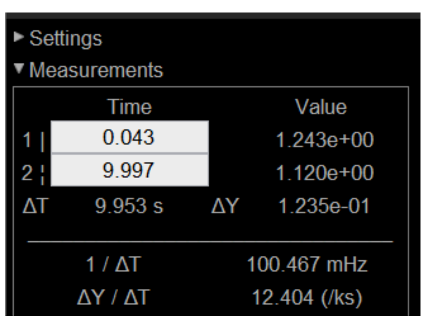

	Time		Value
1	0.043		1.243e+00
2	9.997		1.120e+00
ΔT	9.953 s	ΔY	1.235e-01
	1 / ΔT		100.467 mHz
	ΔY / ΔT		12.404 (/ks)

Figure 5 Current Measurement at Ruler 1 and Ruler 2

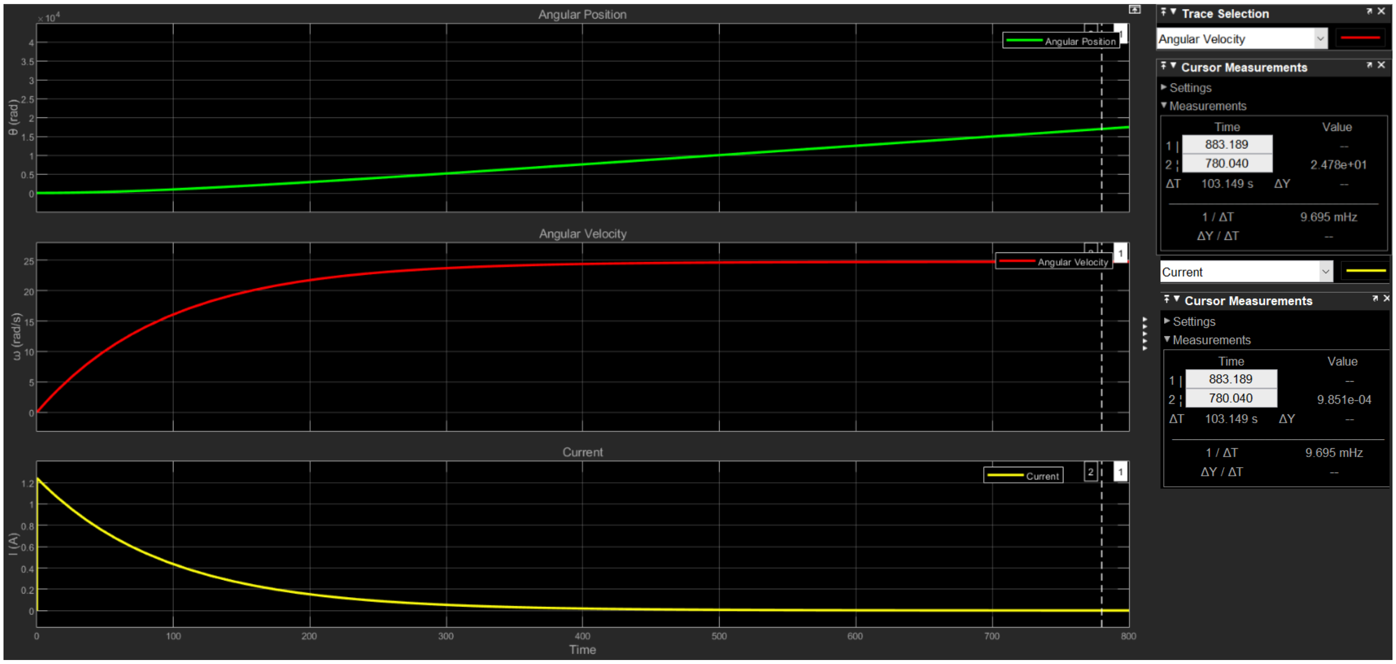

Figure 6 Waveforms of Angular Position, Angular velocity, and Current for 800 seconds

From figure 4, we can see the waveforms of the angular position, angular velocity, and the current. At first, we can see that the current reached a peak to 1.243A at time 0.043 second and decreased to 1.12 at time 9.9 second (Figure 5). If we took the average from these two values then we will get current of 1.18A. The following calculation will show the process:

$$\frac{1.12 + 1.243}{2} = \mathbf{1.18}\boldsymbol{A}$$

For the angular velocity, for the first 10 seconds, the graph was linear and reach 2.5 rad/s at time 10 second. In order to find the maximum angular velocity, we needed to extend the time period to see what will happen to the graph. From Figure 6, it was clearly illustrated that at first the velocity increased significantly from 0 to 16 rad/s within 100 second. However, it started to reach the saturation point below 25 rad/s. From the cursor measurement, at 780 second the speed reached its maximum value of 24.78 rad/s and the current value was almost zero 0.0009851A. This was because of the torque and speed relationship based on figure 21 in appendices. The motor can rotate until this maximum speed if there was no load. During this no-load condition the motor torque will be at rest and due to the equation 4 in method section (Eqn4), motor torque was proportional to the current. Thus, the motor can barely has load at speed of 24.78 rad/s. In addition, the maximum power will occur when the speed is half of the maximum speed, hence at around 12.39 rad/s the maximum power will occur. For the angular displacement, the value increased slowly at first and later it increased linearly versus the time. At time 10 second, the angular displacement reached around 12.5 radian. From figure 6, it also increased linearly versus time and reached around 17000 radians of displacement at time equal to 800 seconds.

b. Changing the payload mass to ($10kg$) and the motor inertia to ($4.3 \times 10^{-4} kgm^2$)

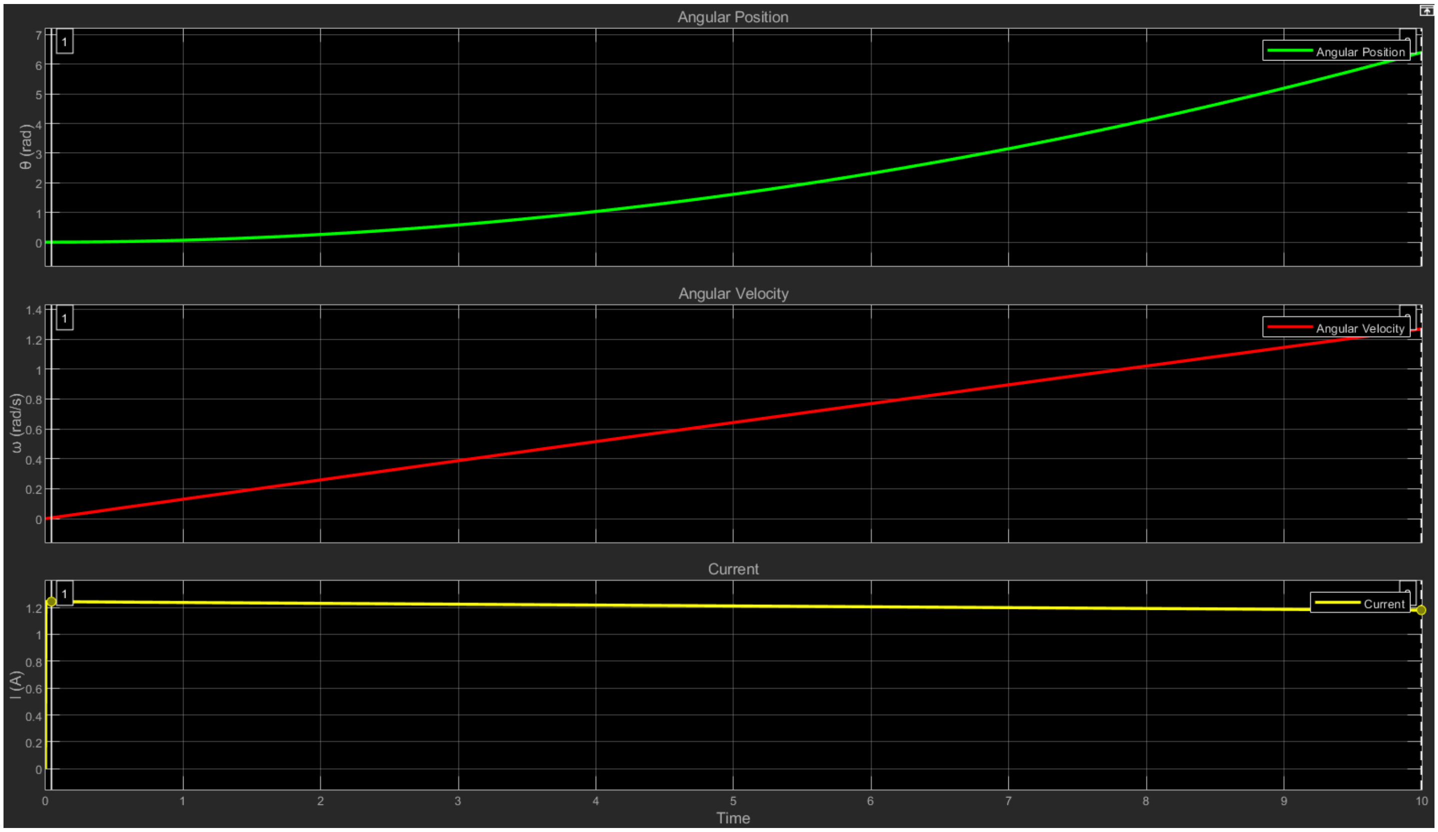

Figure 7 Waveforms of Angular Position, Angular velocity, and Current for 10 seconds with different mass and inertia

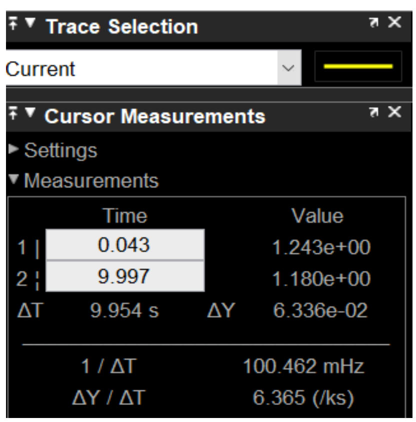

Figure 8 Current Measurement at Ruler 1 and Ruler 2 (with increase payload + inertia)

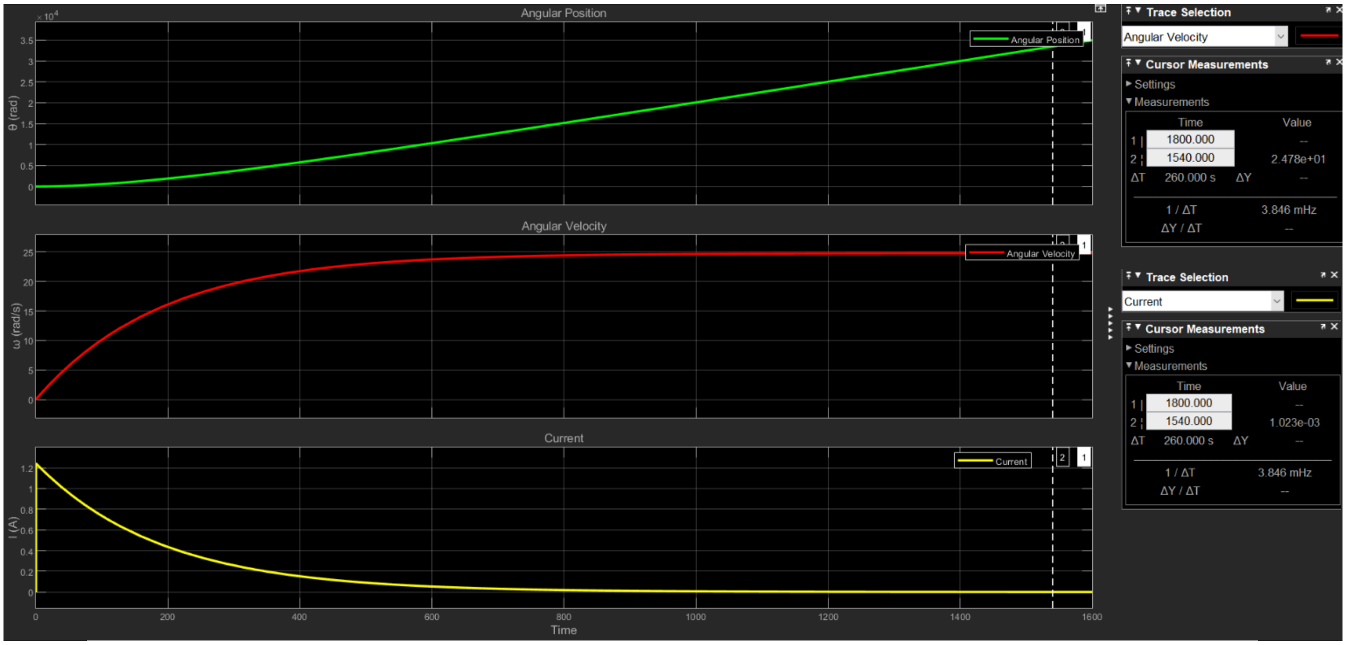

Figure 7 Waveforms of Angular Position, Angular velocity, and Current for 1600 seconds with different mass and inertia

From figure 7, we can see the waveforms of the angular position, angular velocity, and the current. At first, we can see that the current reached a peak to 1.243A at time 0.043 second and decreased to 1.18 at time 9.9 second (Figure 8). If we take the average from these two values then we will get current of 1.15A. The following calculation will show the process:

$$\frac{1.12 + 1.18}{2} = \mathbf{1.15}\boldsymbol{A}$$

For the angular velocity, for the first 10 seconds, the graph was linear and reached 1.3 rad/s at time 10 second. In order to find the maximum angular velocity, we needed to extend the time period to see what will happen to the graph. From Figure 9, it was clearly illustrated that at first the velocity increased significantly from 0 to 7.36 rad/s within 100 second. However, it started to reach the saturation point below 25 rad/s. From the cursor measurement, at 1540 second the speed reached its maximum value of 24.78 rad/s and the current value was almost zero 0.001023. Since the maximum speed was the same with the previous system, the maximum power also occurred at 12.39 rad/s. For the angular displacement, the value increased slowly at first and later it increased linearly versus the time. At time 10 second, the angular displacement reached 6.4 radian. From figure 9, it also incremented linearly versus time and reached around 15000 radians at time equal to 800 second.

2. Close-loop model using Simulink

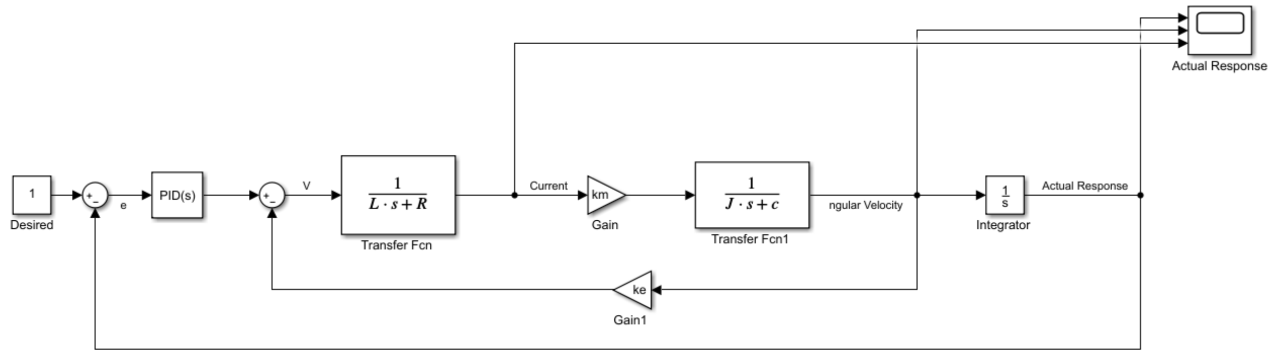

Figure 10 Close Loop System of DC Motor with PID

For the second part (The close loop model using simulink), the input voltage signal was changed to constant value of 1. Then, the actual response value will be fed into the sum block. This block will sum positive value of 1 and negative value of actual response. The result of this arithmetic was passed through PID controller then passed to the sum block of the previous open loop system.

a. Without changing the payload mass ($5kg$) and the motor inertia ($1.3 \times 10^{-4} kgm^2$)

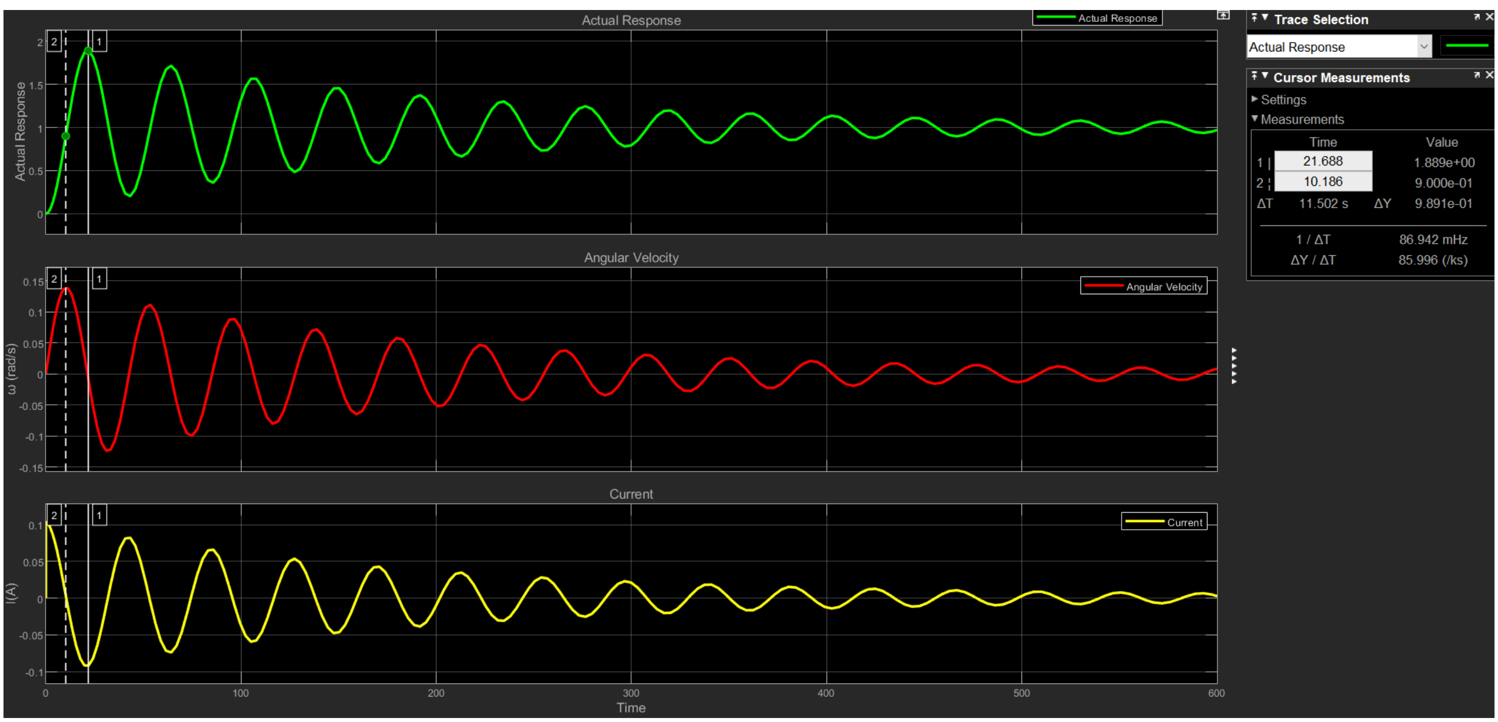

Figure 11 Waveforms of Angular displacement (actual response), Angular Velocity, and Current without PID block

Figure 12 Waveforms of Angular displacement (actual response), Angular Velocity, and Current with PID value from 2c

From figure 11, it was showed clearly that the waveforms of actual response, angular velocity and current were oscillating until the end of simulation (600 second). These three graphs showed that the oscillations were high at the start and the amplitudes were decreasing. It can be seen from the graphs that the reference response for actual response was 1 and for both angular velocity and current were 0. Focusing on the actual response, rise time and peak overshoot were investigated. Rise time was the time it took from the response to rise from 10% to 90% of the final value [2], while peak overshoot is the maximum amount of the response passed the desired value in the first oscillation [3]. It was showed in the cursor measurements that the rise time was around **10 second** and the peak overshoot was **0.889**.

From figure 12, it was showed clearly that the waveforms of actual response, angular velocity and current had dramatic changes at the beginning, had no oscillations and started to go back to their reference value until the end of the simulation (400 second). Focusing on the actual response, it can be seen that the graph was an ideal damping graph, with small peak overshoot of **0.058**, rise time of **10.829 second**, and zero steady state error. This response will reach exactly value of 1 when the time was around 350 second. Thus, the PID values were verified since it generated a desired response (stable close loop system) that still maintained the fast rise time (around 10 second) with small amount of peak overshoot and the elimination of steady state error and unnecessary oscillation.

b. Changing the payload mass to $(10kg)$ and the motor inertia to $(4.3 \times 10^{-4} kgm^2)$

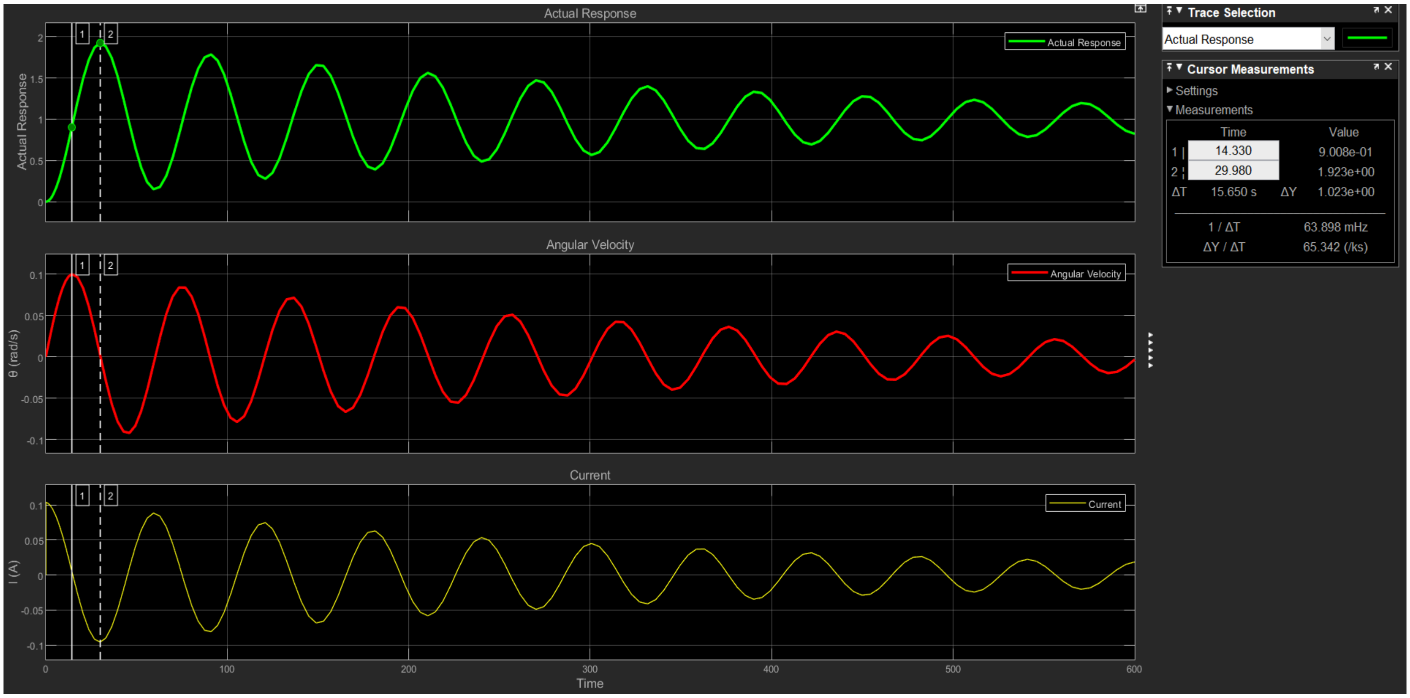

Figure 13 Waveforms of Angular displacement (actual response), Angular Velocity, and Current without PID block (With increase of payload + inertia)

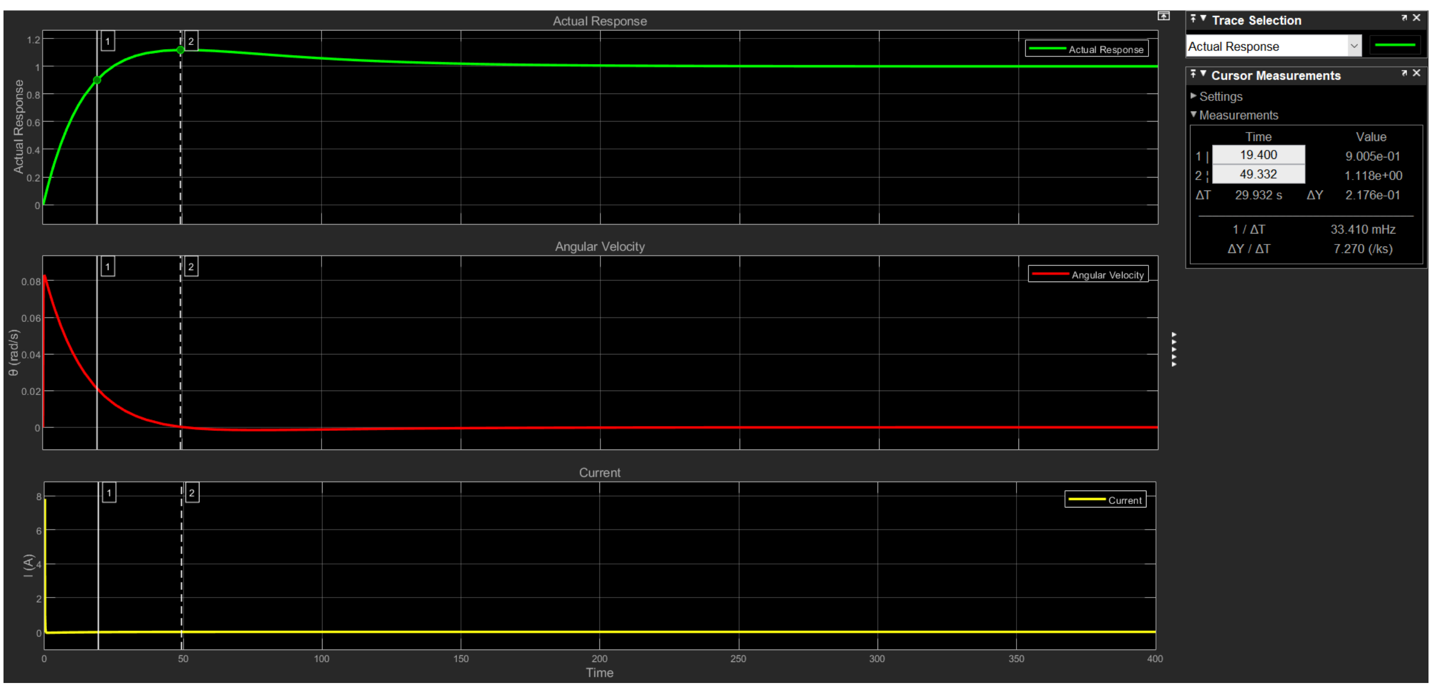

Figure 14 Waveforms of Angular displacement (actual response), Angular Velocity, and Current with PID value from 2c (With increase of payload + inertia)

From figure 13, it was showed clearly that the waveforms of actual response, angular velocity and current were oscillating until the end of simulation (600 second). These three graphs showed that the oscillations were high at the start and the amplitudes were decreasing. It can be seen from the graphs that the reference response for actual response was 1 and for both angular velocity and current were 0. Focusing on the actual response, rise time and peak overshoot were investigated. It was showed in the cursor measurements that the rise time was **14.330 second** and the peak overshoot was **0.923**.

From figure 14, it was showed clearly that the that the waveforms of actual response, angular velocity and current had dramatic changes at the beginning, had no oscillations and started to go back to their reference value until the end of the simulation (400 second). Focusing on the actual response, it can be seen that the graph was an ideal damping graph, with small peak overshoot of **0.118**, rise time of **19.4 second**, and zero steady state error. This response will reach exactly value of 1 when the time was around 700 second (More than the time given in figure 14). Thus, the PID values were verified since it generated a desired response (stable close loop system) that still maintained the fast rise time (around 10 second) with small amount of peak overshoot and the elimination of steady state error and unnecessary oscillation.

c. Setting up the PID parameters

c.1 Without changing the payload mass ($5kg$) and the motor inertia ($1.3 \times 10^{-4} kgm^2$)

The PID values that were chosen for the close loop system with original payload mass and inertia (figure 12) was **Kp = 0.21, Ki = 0.0012, and Kd = 8.32** where Kp is the proportional, Ki is the integral, and Kd is the derivatives.

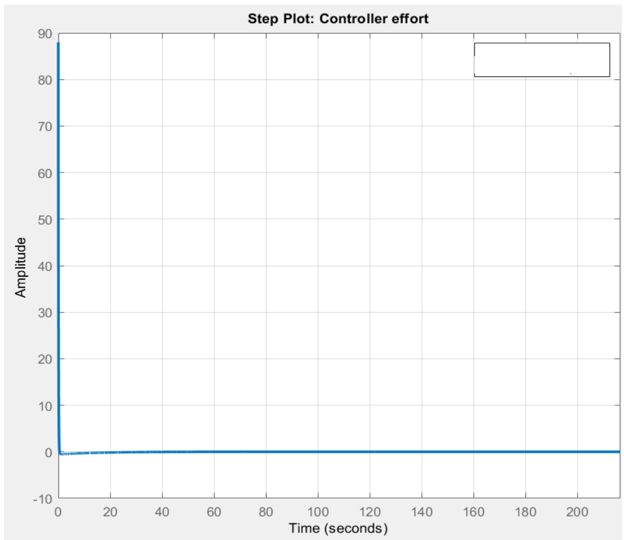

Figure 15 Controller effort for PID for Close Loop System with Original payload mass and inertia

	Recommended PID	Chosen PID
Rise time	65.3 seconds	9.88 seconds
Settling time	604 seconds	103 seconds
Overshoot	12.7 %	5.85 %
Peak	1.13	1.06
Gain margin	100 dB @ 20.8 rad/s	80.9 dB @ 141 rad/s
Phase margin	69 deg @ 0.0212 rad/s	84.3 deg @ 0.182 rad/s
Closed-loop stability	Stable	Stable

Figure 16 Chosen PID Value vs Recommended PID Value (For system with original payload mass and inertia)

These PID Values were analyzed carefully before assigning them for the close loop system. The chosen PID values had an impact for the controller effort. This will make the controller to work harder, it was showed that it reached amplitude of around 88 (Figure 15). Although the recommended PID Values offer controller effort with amplitude that less than 1, it had significant rise time, settling time, and larger overshoot. Thus, the "Chosen PID" was selected since a faster rise time was required for the DC motor plant. In addition, both gain and phase margin values were also far away from negative and these values indicated that the close loop system was far away from instability.

c.2 Changing the payload mass to $(10kg)$ and the motor inertia to $(4.3 \times 10^{-4} kgm^2)$

The PID values that were chosen for the close loop system with original payload mass and inertia (figure 12) was **Kp = 0.173, Ki = 0.00077, and Kd = 7.819** where Kp is the proportional, Ki is the integral, and Kd is the derivatives

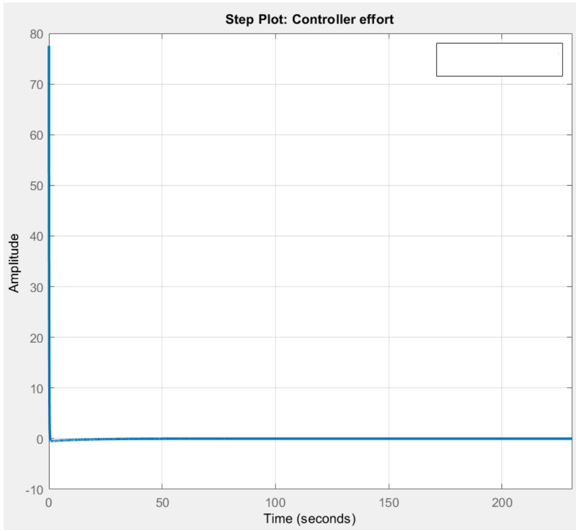

Figure 17 Controller effort for PID for Close Loop System with different payload mass and inertia

	Recommended PID	Chosen PID
Rise time	142 seconds	18 seconds
Settling time	1.55e+03 seconds	147 seconds
Overshoot	10.5 %	11.8 %
Peak	1.1	1.12
Gain margin	106 dB @ 8.14 rad/s	87.5 dB @ 141 rad/s
Phase margin	69 deg @ 0.00923 rad/s	78.5 deg @ 0.0866 rad...
Closed-loop stability	Stable	Stable

Figure 18 Chosen PID Value vs Recommended PID Value (For system with different payload mass and inertia)

These PID Values were selected thoroughly before sending them for the close loop system. The selected PID values had an impact for the controller effort. This will make the controller to work harder, it was proved that it achieved amplitude of around 77 (Figure 17). Although the recommended PID Values offer controller effort with amplitude that less than 1, it had significant rise time and settling time compared to the "Chosen PID". Thus, the "Chosen PID" was selected since a quicker rise time was required for the DC motor plant. In addition, both gain and phase margin values were also far away from negative and these values indicated that the close loop system was far away from instability.

Discussion and Conclusions

From these two open loop systems (Question 1), the current was verified since it reached peak at **1.24A** and has continuous current for around **1.1A.** For the angular velocity, the first open loop system reached **16 rad/s** within the first 100 second, while the second one (with increase mass and inertia) reached **7.36 rad/s**. In addition, the angular velocity will reach maximum value of **24.78 rad/s at 780 seconds** while the other system will take a longer time **(1540 seconds)**. Thus, the increase of payload mass and inertia will lead to slower angular velocity. In addition, the current for both open loop system at 780 and 1540 seconds were almost zero. This verified the torque and speed relationship that the maximum speed will lead to zero torque, hence lead to zero current. For the angular displacement, the first open loop system reached **17000 radians at 800 seconds** while the other system with heavier load reached **15000 radians**. It can be deduced that larger inertia and payload mass will lead the angular displacement to achieve shorter distance. Thus, the angular velocity is proportional to angular displacement, but both are inversely proportional with payload mass and motor inertia.

From these two closed loop systems without PID control, it was clearly seen that the increase in payload mass and inertia will make the system oscillation bigger and longer, hence the rise time was longer, and the overshoot was bigger. These two closed loop systems did not generate the desired response, hence controller was introduced to the close loop system to generate the required response by eliminating the errors. The reason why PID control was selected for this close loop system since it was more flexible than any other controller such as Proportional + Integral controller. PI was not used since derivative control was also needed to deal with motion control such as DC motor system [5]. In addition, based on figure 19 in appendices, PID ability to recover from disturbance was higher than P and PI Controller.

The PID value for the first close loop system with original payload and inertia was **Kp = 0.21, Ki = 0.0012, and Kd = 8.32** and for the second one which slightly lower was **Kp = 0.173, Ki = 0.00077, and Kd = 7.819.** Each of the value was selected carefully since each of them has effect on the rise time, overshoot, settling time, and steady state error [6]. A brief way was to tune the proportional control to reduce the rise time, then tune derivative control to decrease overshoot, and finally tune integral control to reduce steady state error. From figure 12 and 14, both desired responses were obtained with short rise time, small peak overshoot, and zero steady state errors. In addition, the phase and gain margin also indicated a stable system. Thus, the PID values were verified for the close loop system of DC Motor.

References

[1] Seeed Studio. “Choosing the Right Motor for Your Project – DC vs Stepper vs Servo Motors”. Internet: https://www.seeedstudio.com/blog/2019/04/01/choosing-the-right-motor-for-your-project-dc-vs-stepper-vs-servo-motors/ [17 March 2020]

[2] MathWorks. “Stepinfo”. Internet: https://www.mathworks.com/help/control/ref/stepinfo.html [18 March 2020]

[3] John Xu. “Control Design and Implementation Lecture”. *EEEE2056 UNNC*

[4] OptiControls. “Derivative Control Explained”. https://blog.opticontrols.com/archives/153 [18 March 2020]

[5] OptiControls. “PID Controllers Explained”. https://blog.opticontrols.com/archives/344 [18 March 2020]

[6] Control Tutorials for Matlab and Simulink. “Introduction: PID Controller Design”. http://ctms.engin.umich.edu/CTMS/index.php?example=Introduction&section=ControlPID [18 March 2020]

Appendices

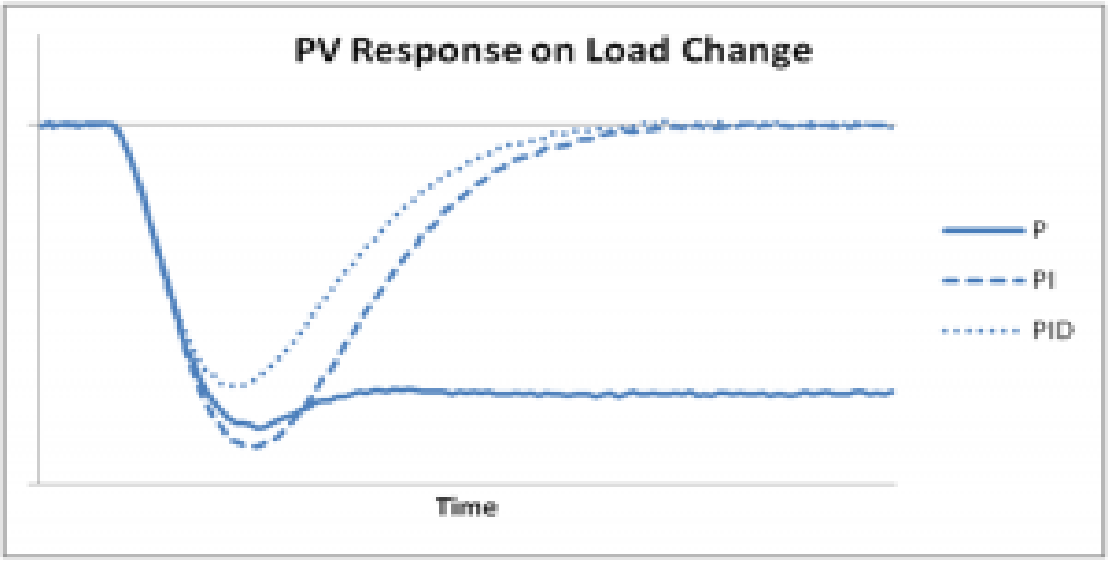

Figure 19 Comparison between P, PI, and PID Controller on Ability to Recover from Disturbance [4]

CL RESPONSE	RISE TIME	OVERSHOOT	SETTLING TIME	S-S ERROR
Kp	Decrease	Increase	Small Change	Decrease
Ki	Decrease	Increase	Increase	Decrease
Kd	Small Change	Decrease	Decrease	No Change

Figure 20 Controller Parameter Effects on Close Loop System [6]

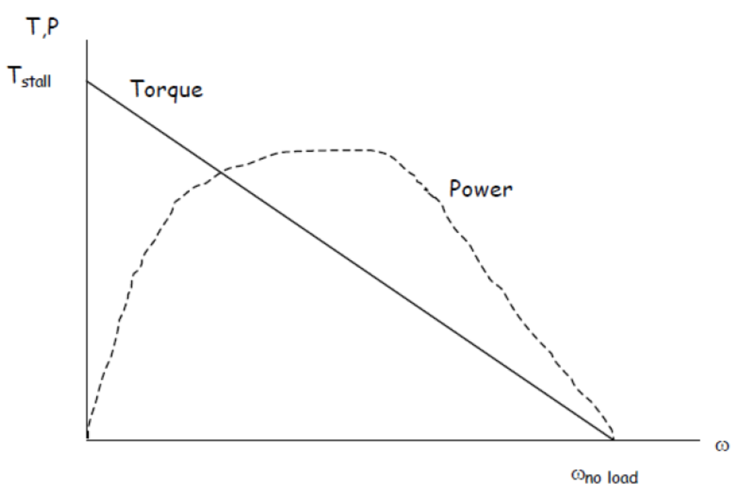

Figure 21 Torque/Speed Relationship